

# Functional Human $\alpha 7$ Nicotinic Acetylcholine Receptor (nAChR) Generated from *Escherichia coli*<sup>§</sup>

Received for publication, March 29, 2016, and in revised form, June 29, 2016. Published, JBC Papers in Press, July 6, 2016, DOI 10.1074/jbc.M116.729970

Tommy S. Tillman<sup>‡</sup>, Frances J. D. Alvarez<sup>§</sup>, Nathan J. Reinert<sup>‡</sup>, Chuang Liu<sup>§</sup>, Dawei Wang<sup>¶</sup>, Yan Xu<sup>‡§¶</sup>, Kunhong Xiao<sup>¶</sup>, Peijun Zhang<sup>§</sup>, and Pei Tang<sup>‡¶||1</sup>

From the Departments of <sup>‡</sup>Anesthesiology, <sup>§</sup>Structural Biology, <sup>¶</sup>Pharmacology and Chemical Biology, and <sup>||</sup>Computational & Systems Biology, University of Pittsburgh School of Medicine, Pittsburgh, Pennsylvania 15260

Human Cys-loop receptors are important therapeutic targets. High-resolution structures are essential for rational drug design, but only a few are available due to difficulties in obtaining sufficient quantities of protein suitable for structural studies. Although expression of proteins in *E. coli* offers advantages of high yield, low cost, and fast turnover, this approach has not been thoroughly explored for full-length human Cys-loop receptors because of the conventional wisdom that *E. coli* lacks the specific chaperones and post-translational modifications potentially required for expression of human Cys-loop receptors. Here we report the successful production of full-length wild type human  $\alpha 7$ nAChR from *E. coli*. Chemically induced chaperones promote high expression levels of well-folded proteins. The choice of detergents, lipids, and ligands during purification determines the final protein quality. The purified  $\alpha 7$ nAChR not only forms pentamers as imaged by negative-stain electron microscopy, but also retains pharmacological characteristics of native  $\alpha 7$ nAChR, including binding to bungarotoxin and positive allosteric modulators specific to  $\alpha 7$ nAChR. Moreover, the purified  $\alpha 7$ nAChR injected into *Xenopus* oocytes can be activated by acetylcholine, choline, and nicotine, inhibited by the channel blockers QX-222 and phencyclidine, and potentiated by the  $\alpha 7$ nAChR specific modulators PNU-120596 and TQS. The successful generation of functional human  $\alpha 7$ nAChR from *E. coli* opens a new avenue for producing mammalian Cys-loop receptors to facilitate structure-based rational drug design.

Human Cys-loop receptors are promising therapeutic targets for various neurological disorders and diseases (1–4). Structure-based drug design for these receptors requires their high-resolution structures (5). Although Cys-loop receptors contain only four major receptor types, including nicotinic acetylcholine receptors (nAChRs),<sup>2</sup> serotonin 5-HT<sub>3</sub> receptors, glycine receptors, and GABA<sub>A</sub> receptors, each receptor type

often has multiple subtypes that form numerous functional distinct receptors. Among the human Cys-loop receptors, high-resolution structures have been obtained for only the  $\beta 3$  GABA<sub>A</sub> and  $\alpha 3$  glycine receptors (6, 7). Structures for other eukaryotic Cys-loop receptors include the mouse serotonin 5-HT<sub>3A</sub> receptor (8), the zebrafish  $\alpha 1$  glycine receptor (9), the *Caenorhabditis elegans* GluCl (10, 11) and the muscle-type nicotinic acetylcholine receptor (nAChR) from *Torpedo marmorata* (12). The dichotomy between the small number of available structures and the relatively large receptor population in the superfamily indicates the technical difficulties for structural determination of these receptors. One of the greatest challenges for structural determination of Cys-loop receptors and similarly complex human membrane proteins is the production of a large quantity of well-folded functional proteins.

The  $\alpha 7$  nAChR ( $\alpha 7$ nAChR) is one of the most abundant nAChR subtypes found in the brain (13, 14). It is also expressed in a wide variety of non-neuronal tissues (15). It has been implicated in diverse biological functions and is an important target for therapeutics (1).  $\alpha 7$ nAChR mostly forms a homo-pentameric ligand-gated ion channel (pLGIC) that conducts calcium and other cations, though heteromeric  $\alpha 7\beta 2$ -nAChR has also been found in both heterologous expression systems and native neurons (16, 17). Structures of the extracellular domain (ECD) and transmembrane domain (TMD) of  $\alpha 7$ nAChR have been determined separately by x-ray crystallography (18) and NMR (19), but the full-length human  $\alpha 7$ nAChR has not previously been obtained from any species in a form suitable for structure determination (20, 21).

Currently available structures for Cys-loop receptors were obtained from proteins expressed in mammalian (6, 8) and insect (7, 9–11, 22) cell lines. We chose an alternate approach: to produce functional full-length human  $\alpha 7$ nAChR in *E. coli*. Production of recombinant proteins in *E. coli* is fast and inexpensive relative to other expression systems. In addition, *E. coli* may produce a more homogeneous population of purified proteins due to its limited ability for post-translational modifications (23). In contrast, the native pathway for  $\alpha 7$ nAChR expression in mammalian cells involves subcellular trafficking through multiple subcellular compartments, where specific chaperone proteins and post-translational modifications aid folding and assembly. Thus,  $\alpha 7$ nAChR purified from mammalian or insect cells contain a mixture of receptors with different post-translational modifications representing various stages of maturation, including glycosylation, palmitoylation, and alternate disulfide conformations (24–26). These modifications

<sup>\*</sup> This work was supported by National Institutes of Health Grant R01GM66358 (to P. T.). The authors declare that they have no conflicts of interest with the contents of this article. The content is solely the responsibility of the authors and does not necessarily represent the official views of the National Institutes of Health.

<sup>§</sup> This article contains supplemental data.

<sup>1</sup> To whom correspondence should be addressed: 2049 Biomedical Science Tower 3, 3501 Fifth Ave., University of Pittsburgh, Pittsburgh, PA 15260. Tel.: 412-383-9798; E-mail: ptang@pitt.edu.

<sup>2</sup> The abbreviations used are: nAChR, nicotinic acetylcholine receptor; pLGIC, pentameric ligand-gated ion channel; ECD, extracellular domain; TMD, transmembrane domain; EM, electron microscopy.

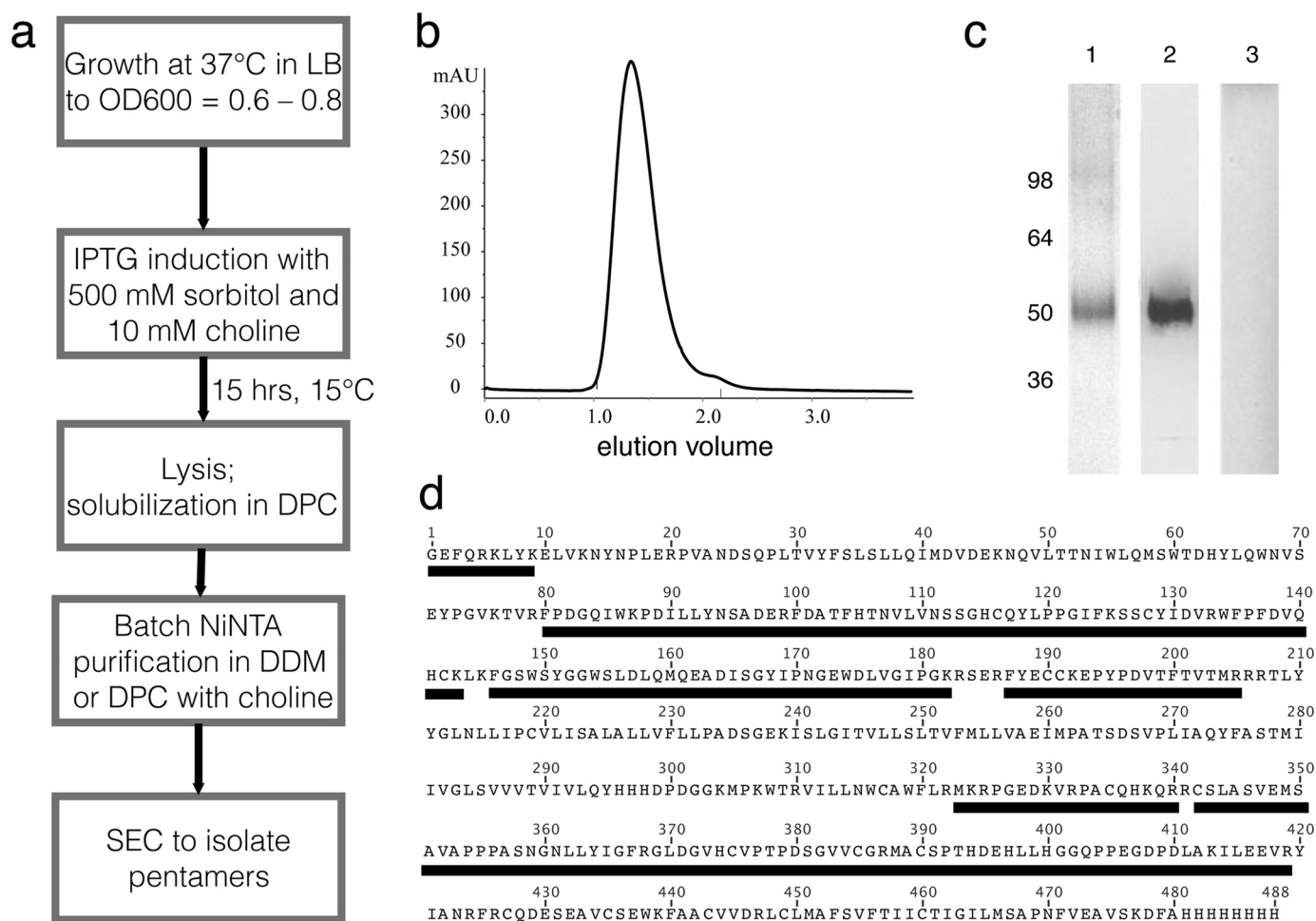


FIGURE 1. Human  $\alpha 7$ nAChR generated from *E. coli*. (a) flowchart providing an overview of  $\alpha 7$ nAChR expression and purification; (b) size exclusion chromatography elution profile of purified  $\alpha 7$ nAChR; (c) Coomassie-stained SDS-PAGE (lane 1) and Western blot identifying purified  $\alpha 7$ nAChR (lane 2) compared with the uninduced control (lane 3); (d) sequence of human  $\alpha 7$ nAChR highlighted with residues identified by mass spectrometry (>51% coverage). Representative mass spectra are provided in the supporting materials.

were reported to be essential for the proper assembly and navigation of functional  $\alpha 7$ nAChR to the mammalian cell surface (24). We hypothesize that these modifications are not needed for the proper folding and pentameric assembly of  $\alpha 7$ nAChR in the simpler expression environment of *E. coli*.

Here we report that  $\alpha 7$ nAChR purified from *E. coli* retains signature properties of native  $\alpha 7$ nAChR, including the ability to assemble into pentameric structures, to bind specific ligands, and to form functional ion channels that can be activated by agonists, inhibited by channel blockers, and enhanced by  $\alpha 7$ nAChR-specific positive allosteric modulators. The study demonstrates that *E. coli* is capable of producing human Cys-loop receptors. It also suggests that the post-translational machinery may not be as essential as previously thought for expressing functional complex membrane proteins.

## Results

**Essential Conditions to Obtain Full-length Human  $\alpha 7$ nAChR from *E. coli***—Our expression construct consists of DNA encoding the wild-type full-length human  $\alpha 7$ nAChR with the signal sequence replaced by that of pelB (a bacterial leader sequence) for expression in *E. coli*. An 8-histidine tag was added to the C

terminus to aid in purification. All subsequent mention of  $\alpha 7$ nAChR refers to this construct. Initial attempts to express full-length human  $\alpha 7$ nAChR in *E. coli* resulted in low expression levels and the formation of inclusion bodies. These problems could not be solved by expression of  $\alpha 7$ nAChR as a fusion protein with MBP, as a chimera with the bacterial homolog ELIC (27) or with various modifications to the protein sequence including codon optimization, deletion of the intracellular loop between the TM3 and TM4 helices, truncation of the N and C termini, and specific mutagenesis of suspected problem sequences.<sup>3</sup> The most significant improvement in the expression of  $\alpha 7$ nAChR was achieved by using osmotic shock (0.5 M sorbitol) at low temperature (15 °C) to induce *E. coli* native chaperones (28) and using the  $\alpha 7$ nAChR agonist choline as a chemical chaperone (29) during induction (Fig. 1a). After testing multiple *E. coli* strains, we found Rosetta(DE3)pLysS to be most suitable for  $\alpha 7$ nAChR expression. For the choice of detergents, we found that *n*-dodecylphosphocholine (DPC) was most effective for extracting  $\alpha 7$ nAChR from cell membranes.

<sup>3</sup> T. S. Tillman and P. Tang, unpublished observations.

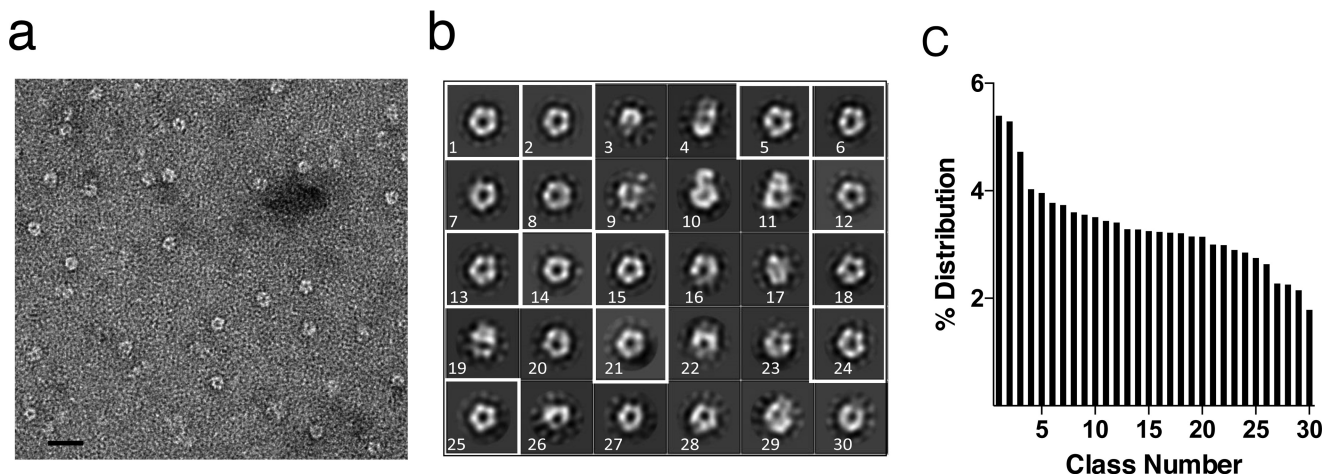


FIGURE 2. **Negative-stain electron microscopy of purified  $\alpha 7$ nAChR demonstrates pentameric assembly.** (a) representative negative-stain image of purified  $\alpha 7$ nAChR. Scale bar, 20 nm; (b) two-dimensional class averages of negative-stain particles. Classes clearly depicting pentamers (white boxes) account for 47% of the particles analyzed; (c) distribution of particles among the class averages.

Both DPC and n-dodecyl  $\beta$ -D-maltoside (DDM) were suitable for purification. Fig. 1*b* shows the size exclusion chromatography (SEC) profile of purified  $\alpha 7$ nAChR, which is consistent with a pentameric assembly. Under these conditions, we can obtain  $1.2 \pm 0.2$  mg pentameric  $\alpha 7$ nAChR from each liter induction culture ( $n = 6$ ). Purified  $\alpha 7$ nAChR migrates on SDS-PAGE with an apparent molecular weight near 50 kDa (Fig. 1*c*), consistent with the de-glycosylated monomer of  $\alpha 7$ nAChR (30). The protein identity was further confirmed by mass spectrometry, which showed more than 51% coverage of tryptic fragments (Fig. 1*d*). Although the C terminus was not identified by mass spectrometry, the full-length  $\alpha 7$ nAChR was ensured by C-terminal His-tag purification. Representative mass spectra are shown in the [supplemental data](#).

**Pentameric Assembly of Purified  $\alpha 7$ nAChR Visualized by EM**—We used electron microscopy (EM) to analyze the oligomeric state of  $\alpha 7$ nAChR. To improve the quality of negative-stain EM images, we reduced excess detergent by exchanging DDM to the chemically similar lauryl maltose neopentyl glycol (LMNG), which forms micelles at very low concentrations (0.01 mM). In the negative-stain EM images,  $\alpha 7$ nAChR was observed as discrete particles (Fig. 2*a*). From 113 micrographs, 7300 particles were sorted into 30 classes by two-dimensional classification (Fig. 2*b*). Among them, at least 13 classes represent essentially different versions of pentameric particles of  $\sim 6$ – $7$  nm in diameter with a pore in the middle (Fig. 2*b*, white box), accounting for 47% of the particles analyzed (Fig. 2*c*). The remaining classes may include various tilted views or aberrant particles. Under these sample conditions,  $\alpha 7$ nAChR appears to prefer an orientation showing the end-on view (*i.e.* top or bottom), precluding three-dimensional reconstruction.

**Purified  $\alpha 7$ nAChR Retains Binding Sites for Bungarotoxin, PNU-120596, and TQS**—Native human  $\alpha 7$ nAChR demonstrates nanomolar binding affinity for the antagonist bungarotoxin (31), and micromolar binding affinity for positive allosteric modulators specific to  $\alpha 7$ nAChR, such as 1-(5-chloro-2,4-dimethoxyphenyl)-3-(5-methyl-1,2-oxazol-3-yl)urea (PNU-120596) (32) and 4-(1-naphthyl)-3a,4,5,9b-tetrahydro-3H-cyclopenta[c]quinoline-8-sulfonamide (TQS) (33).

We measured binding of bungarotoxin to the purified  $\alpha 7$ nAChR immobilized on NiNTA plates using a chemiluminescent assay and found an affinity of  $4 \pm 1$  nM (Fig. 3*a*), which is similar to the reported value of  $\sim 5$  nM measured from  $\alpha 7$ nAChR heterologously expressed in SH-EP1 human epithelial cells (31). Using surface plasmon resonance, we also measured binding affinities of PNU-120596 and TQS to purified  $\alpha 7$ nAChR immobilized on a NiNTA chip (Fig. 3, *b* and *c*). For our purified  $\alpha 7$ nAChR, PNU-120596 had an apparent disassociation constant ( $K_d$ ) of  $1.1 \pm 0.1$   $\mu$ M, which is close to the previously reported half maximal effective concentration ( $EC_{50}$ ) of  $1.6 \pm 0.4$   $\mu$ M (32). TQS has a relatively lower affinity than PNU-120596 with a  $K_d$  of  $7.8 \pm 3.2$   $\mu$ M, which is similar to the  $EC_{50}$  of  $6.2 \pm 0.6$   $\mu$ M reported previously (33). The results provide convincing evidence that human  $\alpha 7$ nAChR purified from *E. coli* retains binding sites for these ligands as observed in native membranes.

**Purified  $\alpha 7$ nAChR Remains Functional**—We measured the functional integrity of purified  $\alpha 7$ nAChR using quantitative bungarotoxin pull-down experiments and electrophysiology measurements in *Xenopus* oocytes.

$\alpha$ -Bungarotoxin binding to  $\alpha 7$ nAChR has been used as a measure of functional  $\alpha 7$ nAChR at the cell surface (34). We found that  $92.9 \pm 0.3\%$  of purified  $\alpha 7$ nAChR was pulled-down by  $\alpha$ -bungarotoxin immobilized to Sepharose resin, as measured by absorbance at  $A_{280}$  ( $n = 3$ ). The result suggests that most of the purified  $\alpha 7$ nAChR is folded properly in an active state.

Oocytes injected with purified  $\alpha 7$ nAChR showed activation currents upon applying the agonist choline, acetylcholine, or nicotine in TEVC experiments (Fig. 4*a*). Note that choline is a selective agonist for  $\alpha 7$ nAChR (35). The observed currents from protein injection ( $6 \pm 2$  nA,  $n = 5$ ) are smaller than currents from cRNA injection ( $150 \pm 50$  nA,  $n = 5$ ). The smaller current is typical for purified channel proteins injected into oocytes (36–38). Oocytes tolerate injection of only a limited amount of reconstituted protein. We injected only 5 ng of purified  $\alpha 7$ nAChR compared with 25 ng of cRNA. Each cRNA molecule can result in hundreds of synthesized protein molecules (39). Therefore, it is anticipated that cRNA injection will gen-



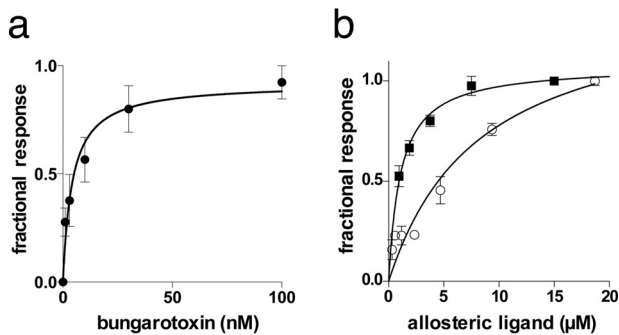


**FIGURE 3. Purified  $\alpha 7$ nAChR retains binding sites for antagonists and positive allosteric modulators.** (a) binding of the competitive antagonist bungarotoxin to purified  $\alpha 7$ nAChR. The data were obtained by chemiluminescence assay ( $n = 3$ ) and fit by nonlinear regression ( $K_d = 4 \pm 1$  nM). (b) binding of positive allosteric modulators PNU-120596 (square) and TQS (circle) to purified  $\alpha 7$ nAChR. The data were obtained by surface plasmon resonance ( $n = 3$ ) and fit by nonlinear regression. The  $K_d$  values for PNU-120596 and TQS are  $1.1 \pm 0.1$   $\mu$ M and  $7.8 \pm 3.2$   $\mu$ M, respectively.

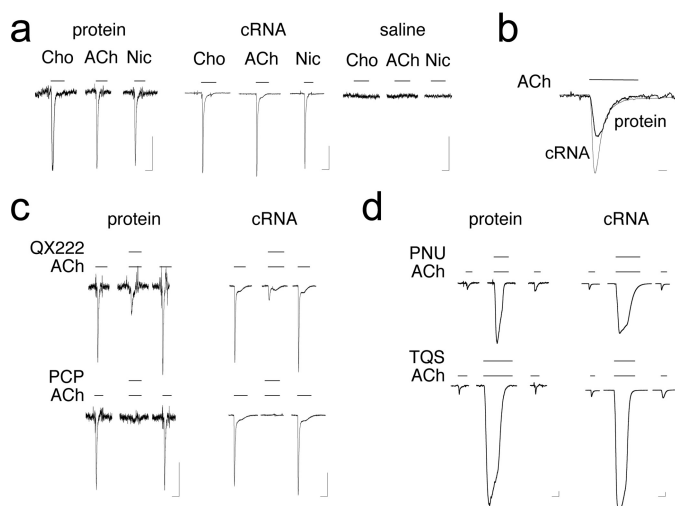


**FIGURE 4. Reconstituted  $\alpha 7$ nAChR forms a functional ion channel.** Channels generated by injecting purified  $\alpha 7$ nAChR (protein) or  $\alpha 7$ nAChR cRNA (cRNA) into oocytes respond similarly to (a) activation by the agonists choline (10 mM), acetylcholine (100  $\mu$ M), and nicotine (100  $\mu$ M). These agonists did not generate current in saline-injected oocytes. (b) channels from protein and cRNA injection showed similar kinetics to activation by acetylcholine (100  $\mu$ M). (c) channels from protein and cRNA injection are inhibited similarly by the channel blockers QX-222 (100  $\mu$ M) and PCP (100  $\mu$ M), and potentiated by (d) PNU-120596 (10  $\mu$ M) and TQS (30  $\mu$ M). The bars over the traces indicate application of the indicated ligands. Vertical scale bars represent 5 nA and 50 nA for protein and cRNA injections, respectively. Horizontal scale bars represent 10 s for all traces except the one in (b) which is 1 s. Traces are representative of  $n = 5$  independent oocytes.

erate many more channels and larger currents than protein injection. The currents were absent from oocytes injected with buffer only (Fig. 4a). Fast activation and desensitization are signature properties of  $\alpha 7$ nAChR (13). An expanded time scale demonstrates similar kinetics for currents resulting from protein and cRNA injections (Fig. 4b). Representative traces in Fig. 4c show that the currents were inhibited by channel blockers *N*-(2,6-dimethyl-phenylcarbamoylmethyl) trimethylammonium chloride (QX-222) (40) ( $79 \pm 3\%$  versus  $74 \pm 5\%$  for protein and cRNA injections, respectively,  $n = 5$ ) and phencyclidine (PCP) (41, 42) ( $92 \pm 2\%$  versus  $93 \pm 3\%$  for protein and cRNA injections, respectively,  $n = 5$ ). Protein- and cRNA-injected oocytes also showed similar potentiation by PNU-120596 ( $9 \pm 3$  versus

$12 \pm 3$  for protein and cRNA injections, respectively,  $n = 5$ ) and TQS ( $18 \pm 5$  versus  $23 \pm 4$  for protein and cRNA injections, respectively,  $n = 5$ ), both of which are  $\alpha 7$ nAChR specific positive allosteric modulators (32, 43). Representative traces are shown in Fig. 4d. These results demonstrate that human  $\alpha 7$ nAChR generated from *E. coli* can form functional channels that retain pharmacological characteristics of native  $\alpha 7$ nAChR.

## Discussion

Among all the members of the Cys-loop superfamily of ligand gated ion channels,  $\alpha 7$ nAChR is known to be particularly difficult to express (20, 21). Its functional expression in mammalian cells is cell-type dependent, which has been linked to the requirement for specific chaperone proteins and post-translational modifications (24). Even in permissive cells, it has been estimated that only 62% of the total  $\alpha 7$ nAChR protein present in the cell is in a mature functional form (31). This may be a problem inherent to heterologous expression in eukaryotic cells, not only for  $\alpha 7$ nAChR but also for other homologous receptors. Indeed, those eukaryotic Cys-loop channels for which structures have been successfully determined have all been mutagenized or processed *in vitro* in an effort to improve monodispersity of the final product (6–11, 22). Production of functional human  $\alpha 7$ nAChR in *E. coli* suggests that specific chaperone proteins and post-translational modifications are not required for channel function, but instead are a consequence of sub-cellular trafficking in eukaryotic cells. Post-translational modification in *E. coli* is limited (23), which may improve homogeneity of the protein expression. Our results show that the *E. coli* chaperones induced by osmotic and cold shock as well as the chemical chaperone choline are sufficient for producing large quantities of well-folded  $\alpha 7$ nAChR.

In addition to the expression conditions, the oligomeric state of  $\alpha 7$ nAChR was sensitive to purification procedures. Under optimal conditions, the pentameric form was stable for 2 or 3 days at 4 °C. However, the isolated pentamer fraction had a tendency to aggregate under conditions of low ionic strength or detergent concentration; or to dissociate to smaller oligomeric structures under conditions of high ionic strength or detergent concentration. The tendency to form multiple oligomeric structures may be an intrinsic property of  $\alpha 7$ nAChR. Metabolically labeled  $\alpha 7$ nAChR obtained from mammalian PC12 cell culture through microscale purification was found to form multiple oligomeric structures (44). A mutated construct of the zebra finch  $\alpha 7$ nAChR expressed in HEK293F cells also showed micro-aggregation by negative-stain EM (45). Our study suggests that homogenous  $\alpha 7$ nAChR can be obtained by carefully controlling the purification conditions and time window.

*E. coli* readily expresses the bacterial homologues of Cys-loop receptors, such as GLIC (46, 47) and ELIC (48). Because of the traditional wisdom that post-translational modification is essential for producing functional eukaryotic channel proteins, using *E. coli* to express mammalian Cys-loop receptors is almost uncharted territory. Our results challenge that traditional wisdom and suggest that careful manipulation of expression conditions can allow production of functional human  $\alpha 7$ nAChR in *E. coli*. It is likely that other members of the Cys-loop receptor superfamily can also be produced from *E. coli*

following similar protocols. Given the pharmaceutical interest in these receptors as therapeutic targets, perhaps their expression in *E. coli* should be revisited.

## Experimental Procedures

**Expression and Purification of Human  $\alpha 7$ nAChR from *E. coli***—Human  $\alpha 7$ nAChR (UniProtKB P36544: ACHA7\_HUMAN) with the pelB leader sequence (removed during expression) and a C-terminal 8-histidine tag was expressed from the T7 promoter using the expression vector pTBSG1 (49). There was no modification to the native  $\alpha 7$ nAChR sequence. The protein was expressed in Rosetta 2(DE3)pLysS (Novagen) using the Marley protocol (50). Induction with 0.2 mM IPTG was for 16 h at 15 °C in LB broth containing 500 mM sorbitol and 10 mM choline. Cells from 1 liter induction medium were resuspended in 25 ml of buffer A containing 50 mM Tris, pH 8, 500 mM NaCl, 500 mM sucrose, 10 mM choline, 10% glycerol, and HALT protease inhibitor. All subsequent operations were at 4 °C. Cells were lysed using an Avestin Emulsi-flex-C3 homogenizer. The cell lysate was adjusted to 0.33% DPC and 20 mM imidazole and incubated for 2 h. The insoluble fraction was then removed by ultracentrifugation (1 h 200 k  $\times$  g) and the supernatant incubated with 3 ml of NiNTA resin (GEHealthcare) for 2 h, mixing by inversion. The resin was transferred to a column and washed with 10 column volumes (cv) of buffer A, followed by 10 cv buffer B containing 100 mM imidazole, 10% glycerol, 150 mM NaCl, and 0.05% DDM.  $\alpha 7$ nAChR was eluted with buffer C containing 250 mM imidazole, 10% glycerol, 150 mM NaCl, and 0.05% DDM. The purified protein was concentrated to 0.5 mg/ml using a Vivaspin 2 molecular weight cut-off 100,000 centrifugal filter (Sartorius, Germany), and the pentamer fraction was isolated by SEC using a S200 10/300 or S200 3.2/300 column (GEHealthcare). Protein purity and identity were assessed by SDS-PAGE and Western blotting analysis, respectively. Western blotting analysis was performed using a monoclonal mouse antibody to the C terminus of  $\alpha 7$ nAChR (catalogue number 60220-1-Ig, Lot number 10001012, ProteinTech). Antibody specificity was confirmed by the manufacturer and by comparison of *E. coli* extracts with and without  $\alpha 7$ nAChR expression.

**Proteomics Analysis to Confirm  $\alpha 7$ nAChR Identity**—Purified  $\alpha 7$ nAChR was digested using an in-solution digestion protocol as described previously (51, 52). Tryptic peptides of  $\alpha 7$ nAChR were injected into a 75  $\mu$ m  $\times$  150 mm BEH C18 column (particle size 1.7  $\mu$ m, Waters), separated using a Waters nanoACQUITY Ultra Performance LC<sup>TM</sup> (UPLC<sup>TM</sup>) System (Waters, Milford, MA) and subjected to LC-MS/MS analyses performed on a Thermo Scientific LTQ Orbitrap XL (Thermo Scientific) with a Finnigan Nanospray II electrospray ionization source in the data dependent mode using the TOP10 strategy (53). In brief, each scan cycle was initiated with a full MS scan of high mass accuracy (400–2,000 *m/z*; acquired in the Orbitrap Elite at 6  $\times$  10<sup>4</sup> resolution setting and automatic gain control (AGC) target of 106), followed by MS/MS scans (AGC target 5,000; threshold 3,000) in the linear ion trap on the 10 most abundant precursor ions. Selected ions were dynamically excluded for 30 s. Singly charged ions were excluded from MS/MS analysis. MS/MS spectra were searched by using the SEQUEST algo-

rithm against a composite database containing the International Protein Index (IPI) (human) protein sequences and their reverse sequences. Search parameters allowed for two missed tryptic cleavages, a mass tolerance of  $\pm 10$  ppm for precursor ion, a mass tolerance of  $\pm 0.02$  Da for product ion, a static modification of 57.02146 Da (carboxyamidomethylation) on cysteine and a dynamic modification of 15.99491 Dalton (oxidation).

**Negative Stain Electron Microscopy and Image Analysis**—To prepare samples for electron microscopy, purified  $\alpha 7$ nAChR was subjected to SEC in 10 mM HEPES pH 7.4, 150 mM NaCl, and 0.002% LMNG. Samples (3  $\mu$ l) from the SEC peak fraction were absorbed to a glow-discharged 400-mesh carbon-coated copper grid. Samples were then stained with two drops of uranyl acetate (2%), blotted with filter paper, and imaged on a TF20 electron microscope (FEI, Hillsboro, OR) equipped with a field emission gun. Images were recorded at  $\times 100,000$  magnification on a 4k  $\times$  4k Gatan Ultrascan CCD camera (Gatan, Warrendale, PA). From 113 micrographs, a total of 7300 particles were picked using EMAN2 (54) and then extracted and classified using Relion 1.4 (55).

**Binding Assays**—A chemiluminescent assay was used to measure binding of biotinylated bungarotoxin to purified  $\alpha 7$ nAChR immobilized on 96-well NiNTA plates (ThermoFisher, Waltham, MA). Briefly, each well was incubated with 30  $\mu$ l 100  $\mu$ g/ml purified  $\alpha 7$ nAChR for 6 h at 4 °C, then washed three times with 50 mM sodium phosphate buffer pH 7.4, 0.025% DDM, 0.05 mg/ml asolectin, followed by another wash with 50 mM sodium phosphate, pH 7.4, 0.1 mg/ml asolectin. Biotin conjugated bungarotoxin (ThermoFisher, Waltham, MA) was added at the indicated concentrations in 50 mM sodium phosphate buffer and incubated overnight at 4 °C. Excess bungarotoxin was removed by three 200- $\mu$ l washes with Tris-buffered saline, 0.05% Tween. Avidin-HRP (ThermoFisher, Waltham, MA) was added to each well at 1  $\mu$ g/ml for 1 h and then developed using SuperSignal West Pico Chemiluminescent Substrate (ThermoFisher, Waltham, MA). Negative controls were treated identically, except no  $\alpha 7$ nAChR was present. For the  $\alpha 7$ nAChR-specific positive allosteric modulators PNU-120596 and TQS, steady-state surface plasmon resonance responses to ligand binding to purified  $\alpha 7$ nAChR as a function of ligand concentration were measured at 25 °C using a Biacore 3000 with the NTA sensor chip (GE Healthcare, Uppsala, Sweden).  $\alpha 7$ nAChR was immobilized to the NTA sensor chip with densities between 1000 and 2000 RU. Responses to ligand binding were measured in phosphate-buffered saline with 0.005% lauryldimethylamine-*N*-oxide and 1% dimethyl sulfoxide at a flow rate of 30  $\mu$ l/min. After reference and buffer subtraction, the steady state regions of each sensogram for PNU-120596 and TQS for a series of concentrations up to the solubility limits of the respective ligand were averaged and used to plot the SPR response (*n* = 3). Dissociation constants were derived by non-linear regression analysis using a Langmuir isotherm equation.

**$\alpha$ -Bungarotoxin-Sepharose Pull-down Experiments**— $\alpha$ -Bungarotoxin Sepharose was prepared by reacting 1 mg of bungarotoxin with 200  $\mu$ l of cyanogen bromide-activated Sepharose (GE Healthcare), and then blocking unreacted sites following

the manufacturer's recommendations. Control-Sepharose was prepared by blocking reactive sites in the absence of  $\alpha$ -bungarotoxin. For each experiment, 3.2 nmol of purified  $\alpha 7$ nAChR was incubated overnight with 20  $\mu$ l each of the control-resin or  $\alpha$ -bungarotoxin-resin. The amount of  $\alpha 7$ nAChR pulled down was measured by the absorbance at 280 nm and reported as the mean ratio of  $\alpha$ -bungarotoxin resin/control resin based on three independent experiments.

**Electrophysiology**—Functional measurements of purified  $\alpha 7$ nAChR injected into *Xenopus* oocytes were performed using two electrode voltage clamp experiments (56). We injected additional oocytes with either saline or cRNA encoding  $\alpha 7$ nAChR as negative and positive controls, respectively. For cRNA injections, 25 ng cRNA for  $\alpha 7$ nAChR was co-injected with 25 ng of cRNA for RIC3 to increase surface expression of  $\alpha 7$ nAChR. For protein injections, the purified pentameric  $\alpha 7$ nAChR was reconstituted into vesicles composed of egg phosphatidylcholine, phosphatidic acid, and cholesterol in a 3:1:1 molar ratio. Detergent was removed using Biobeads SM-2 (Bio-Rad) following the manufacturer's recommendations. 5 ng of reconstituted  $\alpha 7$ nAChR was injected into *Xenopus* oocytes. After 1–2 days, channel function was measured in a 20- $\mu$ l oocyte recording chamber (Automate Scientific) clamped at  $-60$  mV with an OC-725C Amplifier (Warner Instruments). The recording solutions contained 96 mM NaCl, 2 mM KCl, 1.8 mM  $\text{CaCl}_2$ , 1 mM  $\text{MgCl}_2$ , and 5 mM HEPES, pH 7.0 and the indicated concentrations of the agonists acetylcholine, choline, nicotine, the channel blockers QX-222, and PCP, and the  $\alpha 7$ nAChR-specific positive allosteric modulators PNU-120596, and TQS. Data were collected and processed using Clampex 10 software (Molecular Devices).

**Author Contributions**—T. S. T. conducted most of the experiments and analyzed the results. F. J. D. A., C. L., and P. Z. performed the electron microscopy experiments. N. J. R. performed electrophysiology measurements. D. W. and K. X. performed the mass spectroscopy analysis. Y. X. and P. T. designed the project. T. S. T. and P. T. wrote the manuscript. All authors reviewed the results and approved the final version of the manuscript.

## References

- Dineley, K. T., Pandya, A. A., and Yakel, J. L. (2015) Nicotinic ACh receptors as therapeutic targets in CNS disorders. *Trends Pharmacol. Sci.* **36**, 96–108
- Braat, S., and Kooy, R. F. (2015) The GABAA Receptor as a Therapeutic Target for Neurodevelopmental Disorders. *Neuron* **86**, 1119–1130
- Lynch, J. W., and Callister, R. J. (2006) Glycine receptors: a new therapeutic target in pain pathways. *Curr. Opin. Investig. Drugs* **7**, 48–53
- Thompson, A. J., and Lummis, S. C. (2007) The 5-HT3 receptor as a therapeutic target. *Expert. Opin. Ther. Targets* **11**, 527–540
- Anderson, A. C. (2003) The Process of Structure-Based Drug Design. *Chem. Biol.* **10**, 787–797
- Miller, P. S., and Aricescu, A. R. (2014) Crystal structure of a human GABAA receptor. *Nature* **512**, 270–275
- Huang, X., Chen, H., Michelsen, K., Schneider, S., and Shaffer, P. L. (2015) Crystal structure of human glycine receptor- $\alpha 3$  bound to antagonist strychnine. *Nature* **526**, 277–280
- Hassaine, G., Deluz, C., Grasso, L., Wyss, R., Tol, M. B., Hovius, R., Graff, A., Stahlberg, H., Tomizaki, T., Desmyter, A., Moreau, C., Li, X. D., Poitevin, F., Vogel, H., and Nury, H. (2014) X-ray structure of the mouse serotonin 5-HT3 receptor. *Nature* **512**, 276–281
- Du, J., Lü, W., Wu, S., Cheng, Y., and Gouaux, E. (2015) Glycine receptor mechanism elucidated by electron cryo-microscopy. *Nature* **526**, 224–229
- Hibbs, R. E., and Gouaux, E. (2011) Principles of activation and permeation in an anion-selective Cys-loop receptor. *Nature* **474**, 54–60
- Althoff, T., Hibbs, R. E., Banerjee, S., and Gouaux, E. (2014) X-ray structures of GluCl in apo states reveal a gating mechanism of Cys-loop receptors. *Nature* **512**, 333–337
- Unwin, N. (2005) Refined structure of the nicotinic acetylcholine receptor at 4 Å resolution. *J. Mol. Biol.* **346**, 967–989
- Couturier, S., Bertrand, D., Matter, J. M., Hernandez, M. C., Bertrand, S., Millar, N., Valera, S., Barkas, T., and Ballivet, M. (1990) A neuronal nicotinic acetylcholine receptor subunit ( $\alpha 7$ ) is developmentally regulated and forms a homo-oligomeric channel blocked by  $\alpha$ -BTX. *Neuron* **5**, 847–856
- Fabian-Fine, R., Skehel, P., Errington, M. L., Davies, H. A., Sher, E., Stewart, M. G., and Fine, A. (2001) Ultrastructural distribution of the  $\alpha 7$  nicotinic acetylcholine receptor subunit in rat hippocampus. *J. Neurosci.* **21**, 7993–8003
- Zdanowski, R., Krzyzowska, M., Ujazdowska, D., Lewicka, A., and Lewicki, S. (2015) Role of  $\alpha 7$  nicotinic receptor in the immune system and intracellular signaling pathways. *Cent. Eur. J. Immunol.* **40**, 373–379
- Wu, J., Liu, Q., Tang, P., Mikkelsen, J. D., Shen, J., Whiteaker, P., and Yakel, J. L. (2016) Heteromeric  $\alpha 7\beta 2$  Nicotinic Acetylcholine Receptors in the Brain. *Trends Pharmacol. Sci.* **37**, 562–574
- Mowrey, D. D., Liu, Q., Bondarenko, V., Chen, Q., Seyoum, E., Xu, Y., Wu, J., and Tang, P. (2013) Insights into distinct modulation of  $\alpha 7$  and  $\alpha 7\beta 2$  nicotinic acetylcholine receptors by the volatile anesthetic isoflurane. *J. Biol. Chem.* **288**, 35793–35800
- Li, S. X., Huang, S., Bren, N., Noridomi, K., Dellisanti, C. D., Sine, S. M., and Chen, L. (2011) Ligand-binding domain of an  $\alpha 7$ -nicotinic receptor chimera and its complex with agonist. *Nat. Neurosci.* **14**, 1253–1259
- Bondarenko, V., Mowrey, D. D., Tillman, T. S., Seyoum, E., Xu, Y., and Tang, P. (2014) NMR structures of the human  $\alpha 7$  nAChR transmembrane domain and associated anesthetic binding sites. *Biochim. Biophys. Acta* **1838**, 1389–1395
- Aztiria, E. M., Sogayar, M. C., and Barrantes, F. J. (2000) Expression of a neuronal nicotinic acetylcholine receptor in insect and mammalian host cell systems. *Neurochem. Res.* **25**, 171–180
- Dineley, K. T., and Patrick, J. W. (2000) Amino acid determinants of  $\alpha 7$  nicotinic acetylcholine receptor surface expression. *J. Biol. Chem.* **275**, 13974–13985
- Moraga-Cid, G., Sauguet, L., Huon, C., Malherbe, L., Girard-Blanc, C., Petres, S., Murail, S., Taly, A., Baaden, M., Delarue, M., and Corringer, P. J. (2015) Allosteric and hyperekplexic mutant phenotypes investigated on an  $\alpha 1$  glycine receptor transmembrane structure. *Proc. Natl. Acad. Sci. U.S.A.* **112**, 2865–2870
- Cain, J. A., Solis, N., and Cordwell, S. J. (2014) Beyond gene expression: the impact of protein post-translational modifications in bacteria. *J. Proteom.* **97**, 265–286
- Millar, N. S., and Harkness, P. C. (2008) Assembly and trafficking of nicotinic acetylcholine receptors (Review). *Mol. Membr. Biol.* **25**, 279–292
- Drisdell, R. C., Manzana, E., and Green, W. N. (2004) The role of palmitoylation in functional expression of nicotinic  $\alpha 7$  receptors. *J. Neurosci.* **24**, 10502–10510
- Green, W. N., and Millar, N. S. (1995) Ion-channel assembly. *Trends Neurosci.* **18**, 280–287
- Tillman, T. S., Seyoum, E., Mowrey, D. D., Xu, Y., and Tang, P. (2014) ELIC- $\alpha 7$  Nicotinic acetylcholine receptor ( $\alpha 7$ nAChR) chimeras reveal a prominent role of the extracellular-transmembrane domain interface in allosteric modulation. *J. Biol. Chem.* **289**, 13851–13857
- de Marco, A., Vigh, L., Diamant, S., and Goloubinoff, P. (2005) Native folding of aggregation-prone recombinant proteins in *Escherichia coli* by osmolytes, plasmid- or benzyl alcohol-overexpressed molecular chaperones. *Cell Stress Chaperones* **10**, 329–339
- Molinari, E. J., Delbono, O., Messi, M. L., Renganathan, M., Arneric, S. P., Sullivan, J. P., and Gopalakrishnan, M. (1998) Up-regulation of human  $\alpha 7$



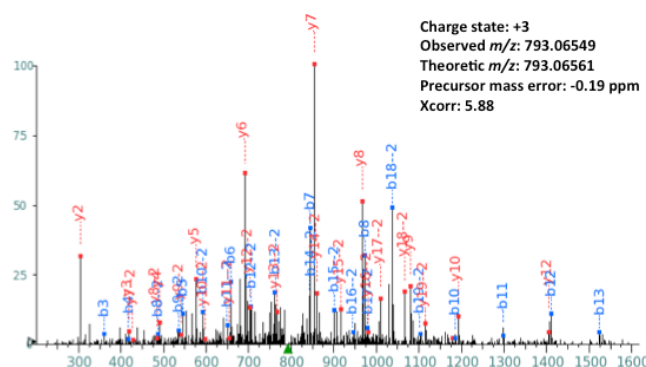
- nicotinic receptors by chronic treatment with activator and antagonist ligands. *Eur. J. Pharmacol.* **347**, 131–139
30. Rangwala, F., Drisdel, R. C., Rakhilin, S., Ko, E., Atluri, P., Harkins, A. B., Fox, A. P., Salman, S. S., and Green, W. N. (1997) Neuronal  $\alpha$ -bungarotoxin receptors differ structurally from other nicotinic acetylcholine receptors. *J. Neurosci.* **17**, 8201–8212
31. Peng, J. H., Fryer, J. D., Hurst, R. S., Schroeder, K. M., George, A. A., Morrissey, S., Groppi, V. E., Leonard, S. S., and Lukas, R. J. (2005) High-affinity epibatidine binding of functional, human  $\alpha 7$ -nicotinic acetylcholine receptors stably and heterologously expressed *de novo* in human SH-EP1 cells. *J. Pharmacol. Exp. Ther.* **313**, 24–35
32. Grønlien, J. H., Håkerud, M., Ween, H., Thorin-Hagene, K., Briggs, C. A., Gopalakrishnan, M., and Malysz, J. (2007) Distinct profiles of  $\alpha 7$  nAChR positive allosteric modulation revealed by structurally diverse chemotypes. *Mol. Pharmacol.* **72**, 715–724
33. Gill, J. K., Savolainen, M., Young, G. T., Zwart, R., Sher, E., and Millar, N. S. (2011) Agonist activation of  $\alpha 7$  nicotinic acetylcholine receptors via an allosteric transmembrane site. *Proc. Natl. Acad. Sci. U.S.A.* **108**, 5867–5872
34. Rakhilin, S., Drisdel, R. C., Sagher, D., McGehee, D. S., Vallejo, Y., and Green, W. N. (1999)  $\alpha$ -bungarotoxin receptors contain  $\alpha 7$  subunits in two different disulfide-bonded conformations. *J. Cell Biol.* **146**, 203–218
35. Alkondon, M., Pereira, E. F., Cortes, W. S., Maelicke, A., and Albuquerque, E. X. (1997) Choline is a selective agonist of  $\alpha 7$  nicotinic acetylcholine receptors in the rat brain neurons. *Eur. J. Neurosci.* **9**, 2734–2742
36. Labriola, J. M., Pandhare, A., Jansen, M., Blanton, M. P., Corringer, P. J., and Baenziger, J. E. (2013) Structural sensitivity of a prokaryotic pentameric ligand-gated ion channel to its membrane environment. *J. Biol. Chem.* **288**, 11294–11303
37. Miledi, R., Palma, E., and Eusebi, F. (2006) Microtransplantation of neurotransmitter receptors from cells to *Xenopus* oocyte membranes: new procedure for ion channel studies. *Methods Mol. Biol.* **322**, 347–355
38. Morales, A., Aleu, J., Ivorra, I., Ferragut, J. A., Gonzalez-Ros, J. M., and Miledi, R. (1995) Incorporation of reconstituted acetylcholine receptors from Torpedo into the *Xenopus* oocyte membrane. *Proc. Natl. Acad. Sci. U.S.A.* **92**, 8468–8472
39. Csárdi, G., Franks, A., Choi, D. S., Airoidi, E. M., and Drummond, D. A. (2015) Accounting for experimental noise reveals that mRNA levels, amplified by post-transcriptional processes, largely determine steady-state protein levels in yeast. *PLoS Genetics* **11**, e1005206
40. Cuevas, J., and Adams, D. J. (1994) Local anaesthetic blockade of neuronal nicotinic ACh receptor-channels in rat parasympathetic ganglion cells. *Br. J. Pharmacol.* **111**, 663–672
41. Connolly, J., Boulter, J., and Heinemann, S. F. (1992)  $\alpha 4-2 \beta 2$  and other nicotinic acetylcholine receptor subtypes as targets of psychoactive and addictive drugs. *Br. J. Pharmacol.* **105**, 657–666
42. Fryer, J. D., and Lukas, R. J. (1999) Noncompetitive functional inhibition at diverse, human nicotinic acetylcholine receptor subtypes by bupropion, phencyclidine, and ibogaine. *J. Pharmacol. Exp. Ther.* **288**, 88–92
43. Hurst, R. S., Hajós, M., Raggenbass, M., Wall, T. M., Higdon, N. R., Lawson, J. A., Rutherford-Root, K. L., Berkenpas, M. B., Hoffmann, W. E., Piotrowski, D. W., Groppi, V. E., Allaman, G., Ogier, R., Bertrand, S., Bertrand, D., and Arneric, S. P. (2005) A novel positive allosteric modulator of the  $\alpha 7$  neuronal nicotinic acetylcholine receptor: *in vitro* and *in vivo* characterization. *J. Neurosci.* **25**, 4396–4405
44. Drisdel, R. C., and Green, W. N. (2000) Neuronal  $\alpha$ -bungarotoxin receptors are  $\alpha 7$  subunit homomers. *J. Neurosci.* **20**, 133–139
45. Cheng, H., Fan, C., Zhang, S. W., Wu, Z. S., Cui, Z. C., Melcher, K., Zhang, C. H., Jiang, Y., Cong, Y., and Xu, H. E. (2015) Crystallization scale purification of  $\alpha 7$  nicotinic acetylcholine receptor from mammalian cells using a BacMam expression system. *Acta Pharmacol. Sin.* **36**, 1013–1023
46. Bocquet, N., Nury, H., Baaden, M., Le Poupon, C., Changeux, J. P., Delarue, M., and Corringer, P. J. (2009) X-ray structure of a pentameric ligand-gated ion channel in an apparently open conformation. *Nature* **457**, 111–114
47. Hilf, R. J., and Dutzler, R. (2009) Structure of a potentially open state of a proton-activated pentameric ligand-gated ion channel. *Nature* **457**, 115–118
48. Hilf, R. J., and Dutzler, R. (2008) X-ray structure of a prokaryotic pentameric ligand-gated ion channel. *Nature* **452**, 375–379
49. Qin, H., Hu, J., Hua, Y., Challa, S. V., Cross, T. A., and Gao, F. P. (2008) Construction of a series of vectors for high throughput cloning and expression screening of membrane proteins from *Mycobacterium tuberculosis*. *BMC Biotechnol.* **8**, 51
50. Marley, J., Lu, M., and Bracken, C. (2001) A method for efficient isotopic labeling of recombinant proteins. *J. Biomol. NMR* **20**, 71–75
51. Kahsai, A. W., Rajagopal, S., Sun, J., and Xiao, K. (2014) Monitoring protein conformational changes and dynamics using stable-isotope labeling and mass spectrometry. *Nat. Protoc.* **9**, 1301–1319
52. Nobles, K. N., Xiao, K., Ahn, S., Shukla, A. K., Lam, C. M., Rajagopal, S., Strachan, R. T., Huang, T. Y., Bressler, E. A., Hara, M. R., Shenoy, S. K., Gygi, S. P., and Lefkowitz, R. J. (2011) Distinct phosphorylation sites on the  $\beta(2)$ -adrenergic receptor establish a barcode that encodes differential functions of  $\beta$ -arrestin. *Sci. Signal* **4**, ra51
53. Haas, W., Faherty, B. K., Gerber, S. A., Elias, J. E., Beausoleil, S. A., Bakalarski, C. E., Li, X., Villén, J., and Gygi, S. P. (2006) Optimization and use of peptide mass measurement accuracy in shotgun proteomics. *Mol. Cell Proteomics* **5**, 1326–1337
54. Tang, G., Peng, L., Baldwin, P. R., Mann, D. S., Jiang, W., Rees, I., and Ludtke, S. J. (2007) EMAN2: an extensible image processing suite for electron microscopy. *J. Struct. Biol.* **157**, 38–46
55. Scheres, S. H. (2012) RELION: implementation of a Bayesian approach to cryo-EM structure determination. *J. Struct. Biol.* **180**, 519–530
56. Dascal, N. (2001) Voltage clamp recordings from *Xenopus* oocytes. *Current Protocols in Neuroscience/ editorial board*, Jacqueline N. Crawley *et al.*, Chapter 6, Unit 6 12

# Functional Human $\alpha 7$ Nicotinic Acetylcholine Receptors from *E. coli*

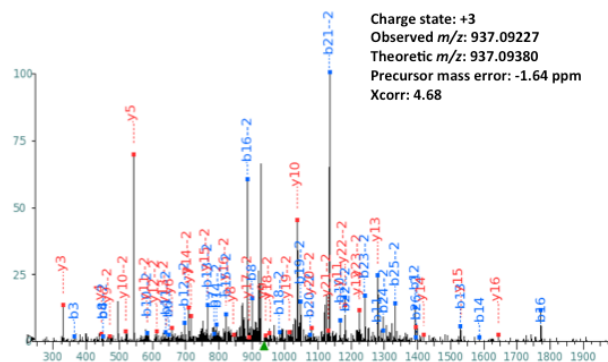
Tommy S. Tillman, Frances J.D. Alvarez, Nathan J. Reinert, Chuang Liu, Dawei Wang, Yan Xu, Kunhong Xiao, Peijun Zhang, and Pei Tang<sup>‡</sup>

**Representative MS/MS spectra** are shown with the identified peptide above the spectra. MS/MS spectra were searched by using the SEQUEST algorithm against a composite database containing the International Protein Index (IPI) (human) protein sequences and their reverse sequences, Identifying human  $\alpha 7$ nAChR with 38.84% coverage. When searched against the human  $\alpha 7$ nAChR sequence, 51.25% coverage was obtained.

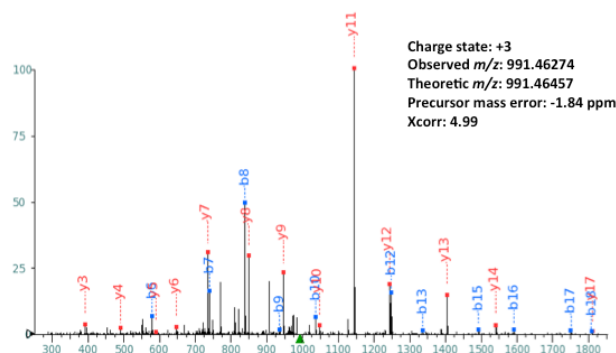
FPDGQIWKPDILLYNSADER



MACSPTHDEHLLHGGQPPEGDPDLAK



GLDGVHCVPTPDGSGVVCGR





**Functional Human  $\alpha 7$  Nicotinic Acetylcholine Receptor (nAChR) Generated from  
*Escherichia coli***

Tommy S. Tillman, Frances J. D. Alvarez, Nathan J. Reinert, Chuang Liu, Dawei Wang,  
Yan Xu, Kunhong Xiao, Peijun Zhang and Pei Tang

*J. Biol. Chem.* 2016, 291:18276-18282.

doi: 10.1074/jbc.M116.729970 originally published online July 6, 2016

---

Access the most updated version of this article at doi: [10.1074/jbc.M116.729970](https://doi.org/10.1074/jbc.M116.729970)

Alerts:

- [When this article is cited](#)
- [When a correction for this article is posted](#)

[Click here](#) to choose from all of JBC's e-mail alerts

Supplemental material:

<http://www.jbc.org/content/suppl/2016/07/06/M116.729970.DC1.html>

This article cites 55 references, 18 of which can be accessed free at  
<http://www.jbc.org/content/291/35/18276.full.html#ref-list-1>